Available online at www.sciencedirect.com
ScienceDirect
Journal of Power Sources 178 (2008) 402–408
JOURNAL OF POWER SOURCES
www.elsevier.com/locate/jpowsour

Effect of binder content on the cycle performance of nano-sized Fe_2O_3-loaded carbon for use as a lithium battery negative electrode

Bui Thi Hang [a,*], Shigeto Okada [b], Jun-ichi Yamaki [b]

[a] *Japan Science and Technology Agency, Kasuga Koen 6-1, Kasuga, Fukuoka 816-8580, Japan*
[b] *Institute for Materials Chemistry and Engineering, Kyushu University, Kasuga Koen 6-1, Kasuga 816-8580, Japan*

Received 15 October 2007; received in revised form 29 November 2007; accepted 3 December 2007
Available online 8 December 2007

Abstract

Nano-sized Fe_2O_3-loaded carbon material was prepared by loading Fe_2O_3 on carbon using various carbonaceous materials. Carbonaceous materials strongly affected the electrochemical behavior of nano-sized Fe_2O_3-loaded carbon. In addition, the binder content also significantly affected the cycle performance of nano-sized Fe_2O_3-loaded carbon. The content of binder depended on the type of carbon used. In the optimal condition for binder content, nano-carbons such as acetylene black (AB), tubular carbon nanofibers (CNF), and platelet CNF provided larger capacities than graphite, and tubular CNF showed the greatest capacity after long-term cycling.

Keywords: Nano-sized Fe_2O_3-loaded carbon material; Binder content; Lithium battery anode

1. Introduction

Over the past few years, iron-based compounds, such as Fe_2O_3, Fe_3O_4, FeOOH, etc., have received increasing attention due to their low cost and low environmental impact [1–12]. Since Larcher et al. [2,3] demonstrated the effect of particle size of the iron oxide on lithium intercalation into α-Fe_2O_3 particles, nano-sized iron oxides have become attractive materials for use in lithium batteries [4–12]. The specific capacity of these materials can be as high as 1000 mAh g^{-1} [13], much higher than graphite, and thus they are promising candidates for use as negative electrode materials in lithium batteries.

In our previous reports [14,15], we stated that nano-sized Fe_2O_3-loaded carbon acted as a rechargeable material in a lithium battery. The carbonaceous materials strongly affected the electrochemical properties of nano-sized Fe_2O_3-loaded carbon [15]. However, the high capacity obtained in the initial cycles rapidly decreased with repeated cycling. To improve the capacity retention, in this study, the effect of binder content on the electrochemical properties of nano-sized Fe_2O_3-loaded carbon was examined to find the optimal binder content as well as the most suitable carbon for use as a high-capacity lithium battery negative electrode.

2. Experimental

Various nano-carbons containing acetylene black (AB, Denki Kagaku Co.) with average diameters of ca. 100 nm and two kinds of carbon nanofibers (CNFs), a nanotube type, with an average diameter of ca. 50 nm, and a platelet type, with an average diameter of ca. 150 nm, were used in the present work. For tubular CNF, graphene is aligned parallel to the fiber axis while in platelet CNF graphene is aligned perpendicular to the fiber axis. For comparison, natural graphite (Chuetsu Graphite Co.), with an average diameter of ca. 18 μm, was also used. The main characteristics and TEM images of the carbon materials used have been described previously [14,15]. Iron nitrate (Wako Pure Chemical, Co.) was used as the iron source.

Nano-sized Fe_2O_3-loaded carbon material was prepared by loading Fe_2O_3 on carbon, as described below. $Fe(NO_3)_3$ was impregnated on carbon with an iron-to-carbon weight ratio of 1:8 in an aqueous solution, and the mixture was dried at 70 °C. This was followed by calcination for 1 h at 400 °C in flowing Ar. The iron compound obtained on the carbon materials was identified to be Fe_2O_3 by X-ray diffraction (XRD). The actual

* Corresponding author. Tel.: +81 92 583 7791; fax: +81 92 583 7791.
E-mail address: hang@cm.kyushu-u.ac.jp (B.T. Hang).

0378-7753/$ – see front matter © 2008 Elsevier B.V. All rights reserved.
doi:10.1016/j.jpowsour.2007.12.001

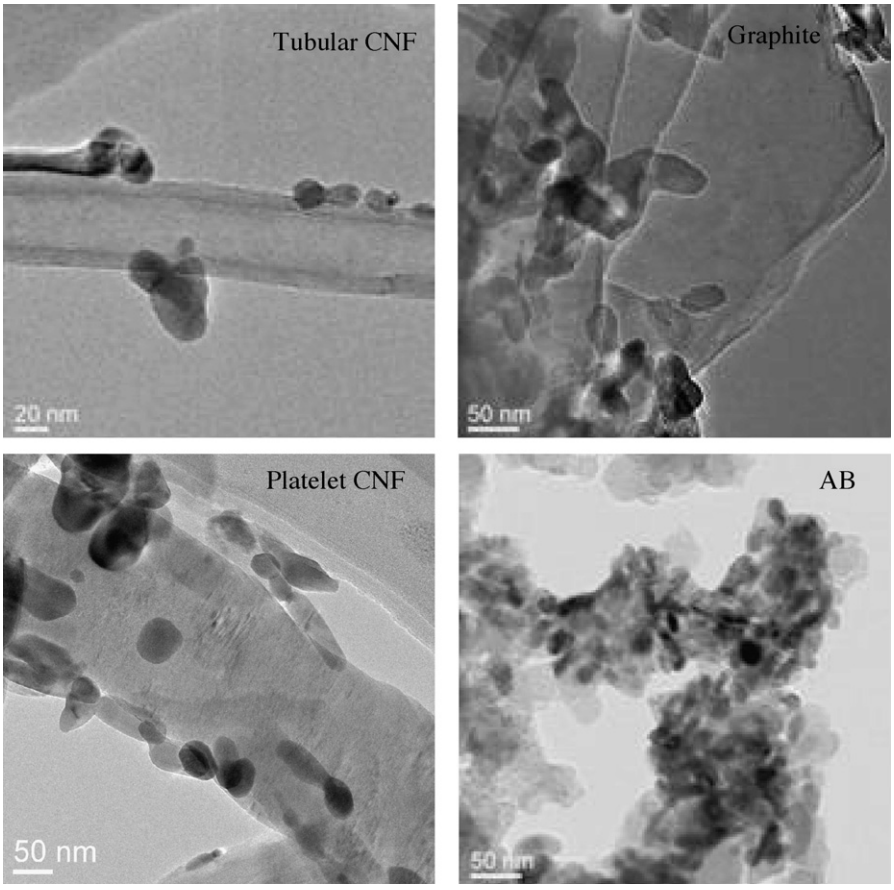

Fig. 1. TEM images of the as-prepared nano-sized Fe_2O_3-loaded carbon materials.

weight ratio of iron to carbon in the obtained materials was checked by the polarized Zeeman atomic absorption spectrophotometer (PZAAS) method. The morphology of the as-prepared nano-sized Fe_2O_3-loaded carbon materials was observed by transmission electron microscopy (TEM) using a Tecnai F20.

All electrochemical measurements were performed at 25 °C using a coin cell with lithium metal as a counter electrode. The working electrode was prepared by mixing nano-sized Fe_2O_3-loaded carbon and polyvinylidene fluoride (PVdF) binder (KF#9100, Kureha Chemical) dissolved in 1-methyl-2-pyrrolidinone (NMP). The content of binder was changed from 10 wt% to 40 wt% depending on the type of carbon. The slurry was applied to the copper current collector. The coated films were dried and cut to 15 mm in diameter. To evaluate the contribution of carbon to the capacity of nano-sized Fe_2O_3-loaded carbons, carbon electrodes without Fe_2O_3 were

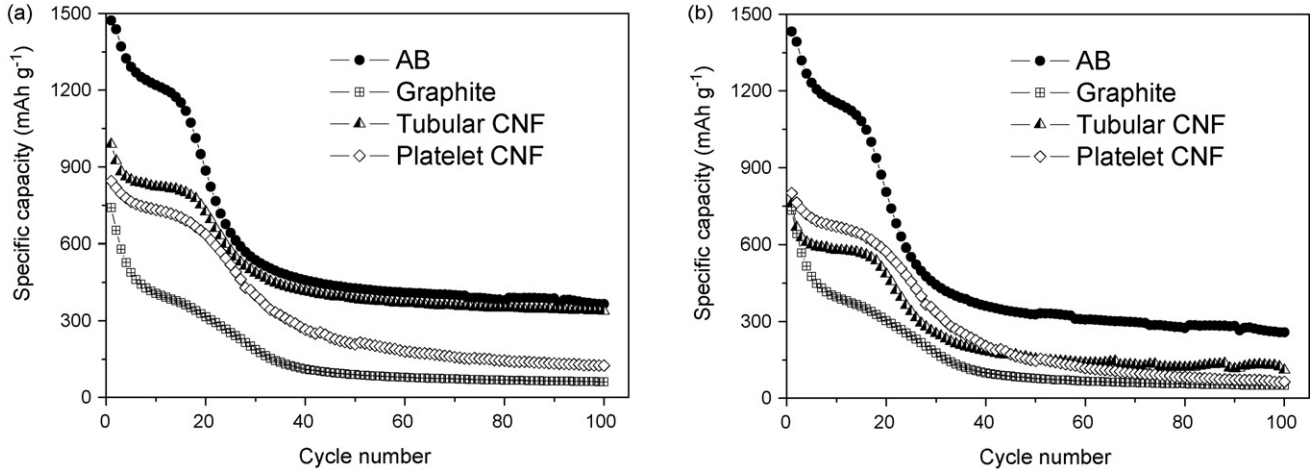

Fig. 2. Cycle performance of nano-sized Fe_2O_3-loaded carbon with 10% PVdF. (a) including contribution of carbon and (b) after subtracting the contribution of carbon.

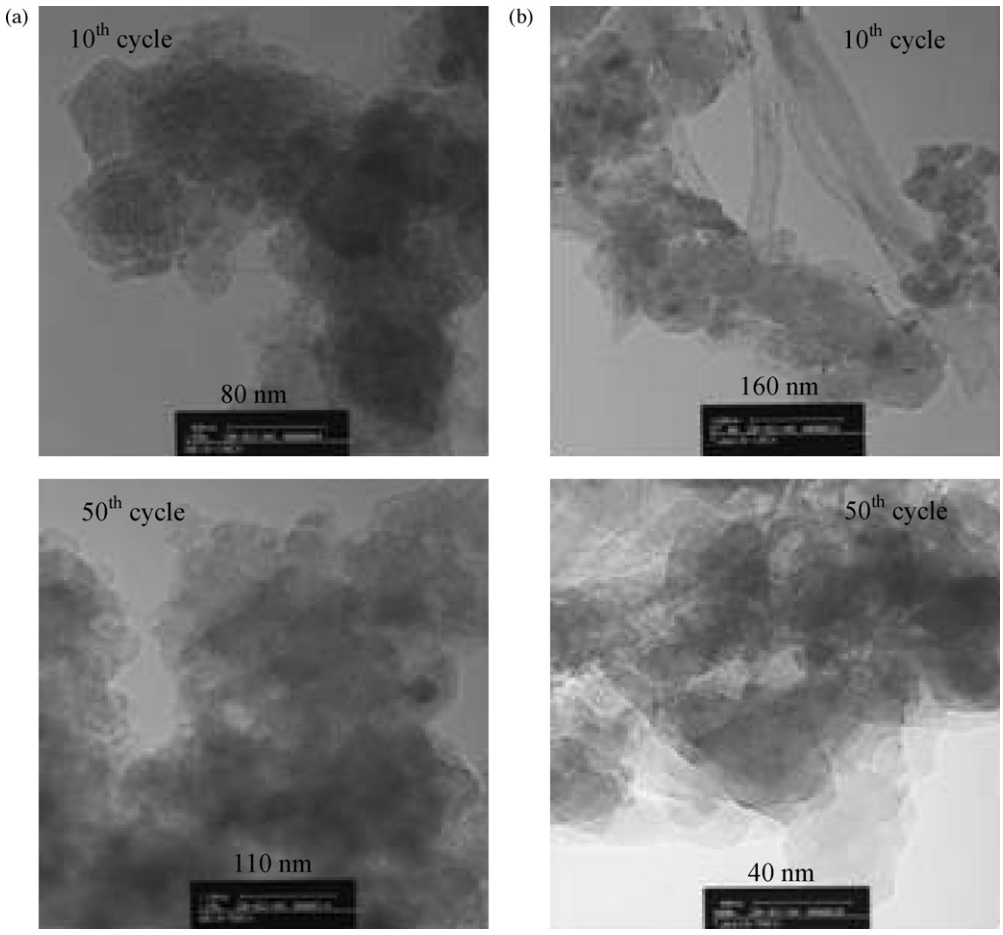

Fig. 3. TEM images of nano-sized Fe_2O_3-loaded (a) AB and (b) tubular CNF after the 10th and 50th cycles.

prepared by the same procedure. These electrodes were then dried for 12 h at 120 °C in a vacuum oven. The cells were assembled in an argon-filled glove box. The electrolyte and separator were 1 M $LiPF_6$ in EC–DMC 1:1 by volume (Tomiyama Pure Chemical Co.) and porous polypropylene (Celgard #3501), respectively. Charge–discharge cycle tests of the coin cells were conducted at a constant current density of 0.2 mA cm^{-2} and within a voltage range of 0.5–3.0 V using a cell-cycling device (Nagano Co.).

3. Results and discussion

TEM images of as-prepared Fe_2O_3-loaded carbons are shown in Fig. 1. The dark particles in the figure are Fe_2O_3. The TEM images demonstrated that fine Fe_2O_3 particles were dispersed on the carbon surface. The particle size of Fe_2O_3 is about a few tenths of a nanometer. Fe_2O_3 particles dispersed on tubular CNF and AB are smaller than those on platelet CNF and graphite. Such dispersion should increase the surface area of active material and improve the redox reaction of iron oxide.

The cycle performance of nano-sized Fe_2O_3-loaded carbon with 10 wt% PVdF is shown in Fig. 2. All of the electrodes showed large reversible capacities in the initial 20 cycles. However, the capacities then rapidly decreased and reached stable values. The stable specific capacities obtained are relatively small compared to those seen in the initial cycles. It is important to find the reason for the onset of the fading in capacity. The cycled cells were disassembled after the 10th and 50th cycles to check the morphology of the working electrode. We found that the material was easily separated from the copper collector when nano-carbons were used. This suggested that 10% PVdF binder may not be sufficient for nano-carbons, which have a greater actual surface area than graphite. To confirm this point, nano-sized Fe_2O_3-loaded AB and tubular CNF were subjected to TEM measurements after the 10th and 50th cycles. The results are shown in Fig. 3. TEM images of cycled samples indicated that the morphology of iron and carbon species was changed compared to that before cycling (Fig. 1). This indicated that the structure of the electrode changed during cycling, perhaps due to insufficient binder content to connect all of the pieces in the electrode. Therefore, during cycling, the change in electrode structure led to a rapid decrease in capacity. In addition, the decrease in capacity may involve the formation of an SEI layer on the surface of the electrode.

To confirm the above supposition, various binder contents were used with all of the carbons and the results are shown in Figs. 4a–7a. For the graphite (Fig. 4a), a binder content higher than 10 wt% does not seem to be beneficial with prolonged cycling. Thus, 10 wt% PVdF gives the best results for nano-sized Fe_2O_3-loaded graphite.

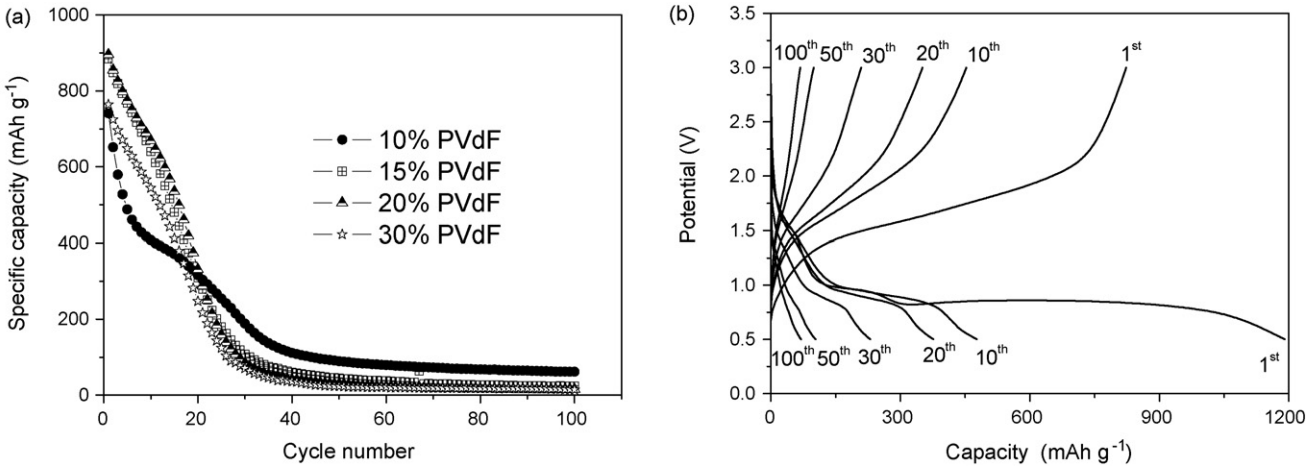

Fig. 4. Cycle performance of nano-sized Fe_2O_3-loaded graphite with various contents of PVdF binder (a) and charge–discharge profiles at the optimal binder content of 10% PVdF (b). (Including contribution of carbon).

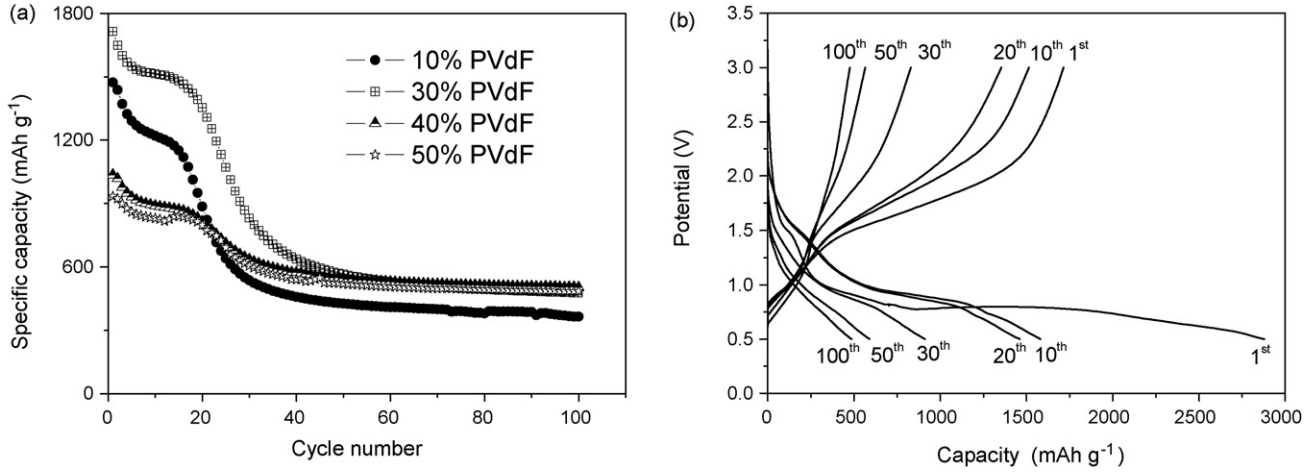

Fig. 5. Cycle performance of nano-sized Fe_2O_3-loaded AB with various contents of PVdF binder (a) and charge–discharge profiles at the optimal binder content of 30% PVdF (b). (Including contribution of carbon).

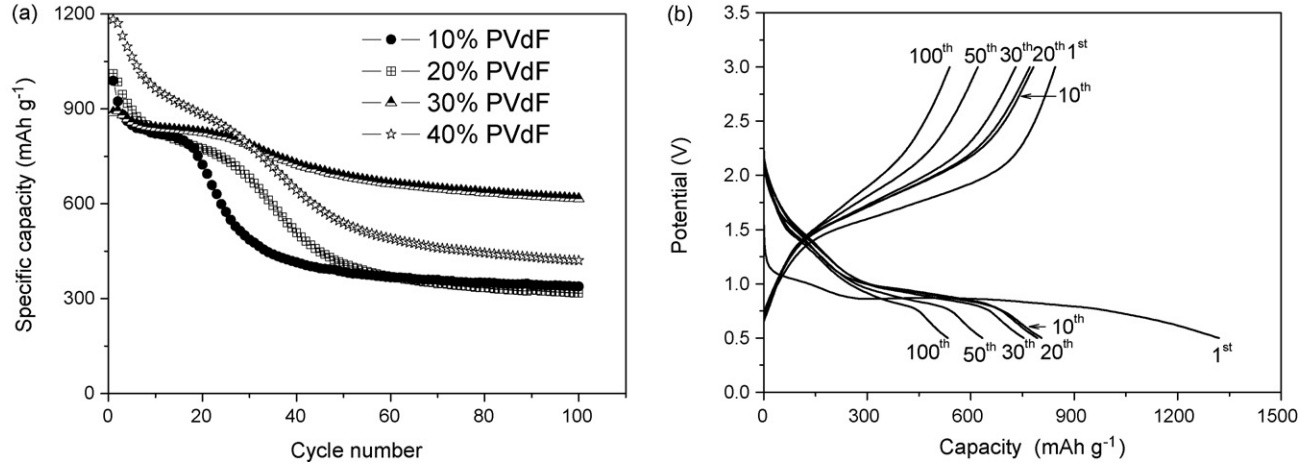

Fig. 6. Cycle performance of nano-sized Fe_2O_3-loaded tubular CNF with various contents of PVdF binder (a) and charge–discharge profiles at the optimal binder content of 30% PVdF (b). (Including contribution of carbon).

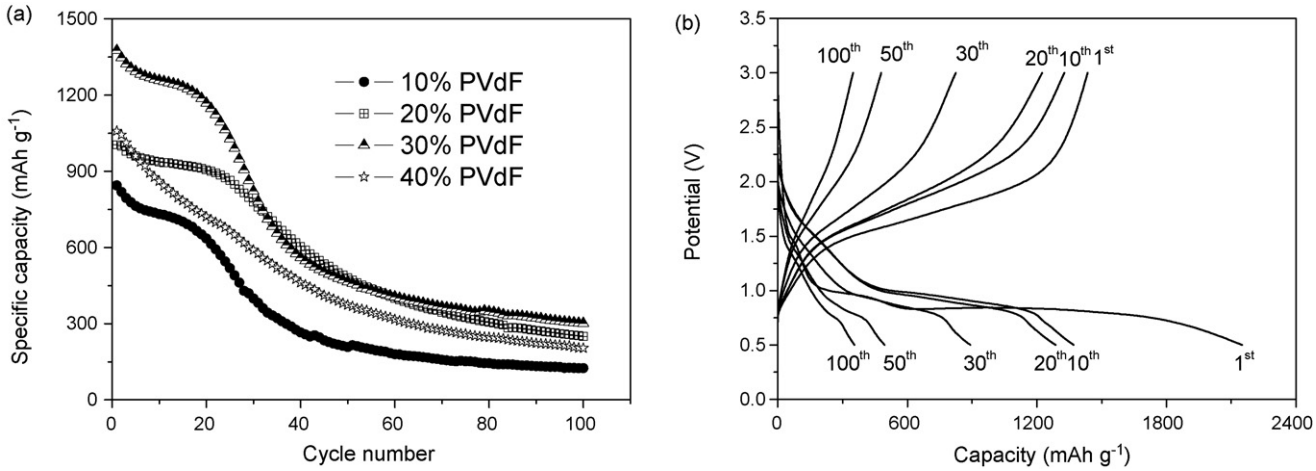

Fig. 7. Cycle performance of nano-sized Fe_2O_3-loaded platelet CNF with various contents of PVdF binder (a) and charge–discharge profiles at the optimal binder content of 30% PVdF (b). (Including contribution of carbon).

In the case of AB (Fig. 5a), when the binder content increased to 30 wt%, while a higher capacity was obtained in the initial cycles, it still rapidly decreased with further cycling. With a further increase in binder content up to 40 wt% or 50 wt%, the capacity decreased. Consequently, for nano-sized Fe_2O_3-loaded AB, the optimal PVdF content seems to be 30 wt%.

With carbon nanofibers such as tubular CNF (Fig. 6a) and platelet CNF (Fig. 7a), the PVdF binder content was changed from 10 wt% to 40 wt% and the capacity significantly improved at a binder content higher than 10 wt%. Among the binder contents used, 30 wt% gave the best results for both tubular CNF and platelet CNF.

The charge–discharge curves of nano-sized Fe_2O_3-loaded carbons using various carbons at the optimal binder content are also shown in Figs. 4b–7b. There is a long voltage plateau at about 0.9 V during the first charge (reduction of Fe_2O_3), but this disappears in subsequent cycles. Such profiles are characteristic of non-intercalated metal oxide electrodes [2,6,8,10–12].

Carbonaceous materials also contributed to the capacity of the electrode, however, the capacity caused by the reaction of lithium with carbon is very small compared to that of nano-sized Fe_2O_3-loaded carbon electrodes, as shown in Fig. 8. The capacity of all the electrodes after subtracting the contribution

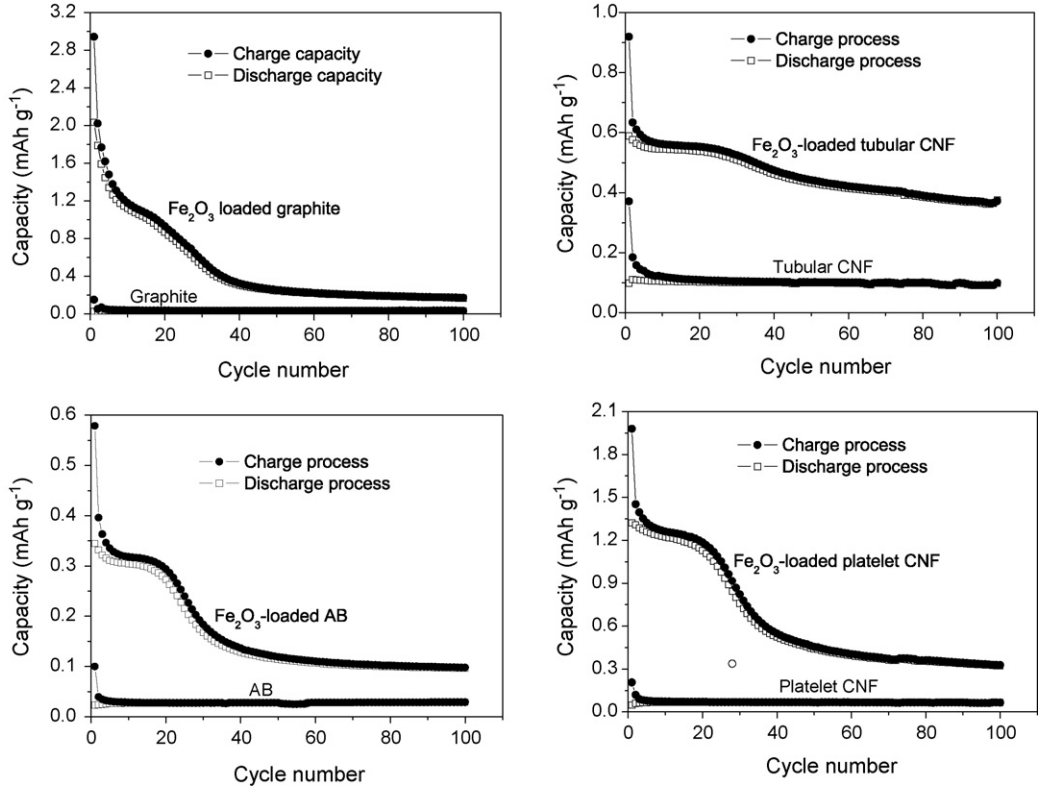

Fig. 8. Cycle performance of carbon and nano-sized Fe_2O_3-loaded carbon at the optimal binder content.

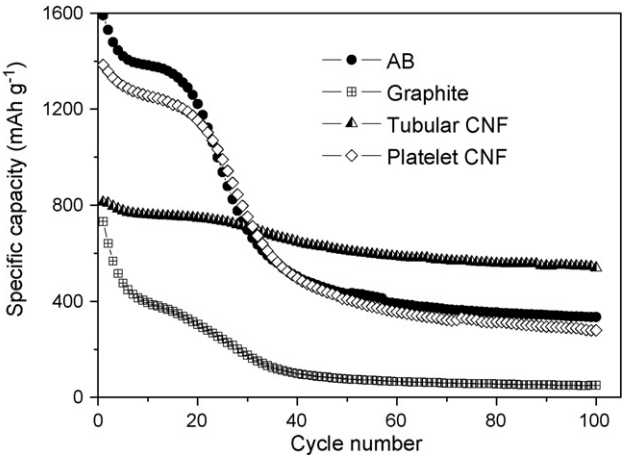

Fig. 9. Cycle performance of nano-sized Fe_2O_3-loaded carbon at the optimal binder content.

of carbon is shown in Fig. 9. In the initial cycles, electrodes that used AB and platelet CNF provided large capacities, even larger than the theoretical capacity of Fe_2O_3 (1005 mAh g^{-1}), but the capacity still rapidly faded after about 20 cycles. This phenomenon was also seen with Fe_2O_3-loaded graphite with a lower capacity. For Fe_2O_3-loaded tubular CNF, the cycle performance was significantly improved. The large observed excesses in capacity can be ascribed to the formation of an organic layer deposited on the surface of metallic iron particles [2]. This has also been observed in α-Fe_2O_3 and Li–Fe oxide [12] and in Li–CoO [16,17]. Thus, the onset of the fading of capacity involved not only the binder but also other factors. One possibility may contribute to the decrease in capacity of electrodes that is SEI layer formed on the electrode surface during cycling. Carbonaceous materials strongly affected particles size and distribution of the Fe_2O_3 on carbon in nano-sized Fe_2O_3-loaded carbon and thus, strongly affected the SEI layer formed during cycling. In the case of nano-carbons, which have a greater surface area than graphite [14,15], iron oxide particles are more dispersed than on graphite, resulting in a greater surface area of iron oxide on nano-carbons. Thereby, nano-sized Fe_2O_3-loaded nano-carbons provide a higher capacity than nano-sized Fe_2O_3-loaded graphite. On the other hand, SEI layer should be thinner on Fe_2O_3-loaded nano-carbons than on Fe_2O_3-loaded graphite and hence the rate of decrease in capacity of Fe_2O_3-loaded nano-carbons electrode was smaller than that of Fe_2O_3-loaded graphite. As for the electrochemical mechanism, Thackeray et al. [18,19] suggested that Li initially intercalates into the α-Fe_2O_3 fcc lattice during the discharging step, and then the Fe is driven out from the lattice to form nano-Fe clusters in a Li_2O matrix at the end of discharge. During the subsequent charging step, the nano-Fe clusters are oxidized back into Fe_2O_3. When SEI formed, Fe and Li_2O were gradually separated, discharge reaction was inhibited and capacity gradually decreased. With further cycling, Fe and Li_2O were more separated by SEI film and after long cycle almost no discharge reaction occurs resulting rapidly decrease in capacity.

A comparison of the cycle performance of nano-sized Fe_2O_3-loaded carbon at the optimal PVdF content (Fig. 9) to that at 10 wt% PVdF (Fig. 2b) suggested that the capacities of the electrodes at the optimal PVdF content were significantly improved.

One possible reason is that Li_2O and Fe particles were not separated when large binder contents were used. As seen on Figs. 4–7, binder contents used depend on the carbonacious materials. When nano-carbons used, due to the larger surface area and more dispersion of Fe_2O_3 particles, the binder contents were larger than graphite. With increasing the binder amount, nano-Fe clusters in a Li_2O matrix will be covered by binder, and separation is difficult to occur.

In addition to binding all of the pieces in the electrode, PVdF plays an important role similar to an agent that accelerates the growth of a gel-like organic layer on the iron particles. In the case of nano-carbons, which have a large actual surface area, nano-Fe_2O_3 was more dispersed on the carbon surface than graphite, and hence the organic layer was larger. An increase in binder content may support the growth of a gel-like organic layer on the iron particles, which leads to an increase in capacity. However, with the formation of SEI layer, the fading of capacity still occur. Among the carbons used, tubular CNF provided the largest capacity after long-term cycling, and is a promising candidate for use as a lithium battery negative electrode.

4. Conclusion

Nano-sized Fe_2O_3-loaded carbon materials using various carbons act as rechargeable electrode materials in a lithium cell. Carbonaceous materials strongly affected the cycle performance of the electrode. High capacities were observed for all of the electrodes in the initial cycles and the capacities then gradually decreased when 10 wt% PVdF was used. An increase in the binder content improved cycle performance for nano-sized Fe_2O_3-loaded carbon electrodes, and the optimal binder content for each carbon was defined. The improvement in capacity was ascribed to the improvement in contact between Fe and Li_2O and the growth of an organic layer on the surface of iron particles when the binder content increased. At the optimal PVdF content, Fe_2O_3-loaded tubular CNF showed the smallest decrease in capacity after long-term cycling, and thus is an interesting candidate for use in a high-capacity lithium-ion battery negative electrode.

Acknowledgement

This work was supported by the CREST program of JST (Japan Science & Technology Agency).

References

[1] K. Amine, H. Yasuda, M. Yamachi, J. Power Sources 81/82 (1999) 221–223.
[2] D. Larcher, C. Masquelier, D. Bonnin, Y. Chabre, V. Masson, J.B. Leriche, J.M. Tarascon, J. Electrochem. Soc. 150 (2003) A133–A139.
[3] D. Larcher, D. Bonnin, R. Cortes, I. Rivals, L. Personnaz, J.M. Tarascon, J. Electrochem. Soc. 150 (2003) A1643–A1650.
[4] G. Jain, C.J. Capozzi, J.J. Xu, J. Electrochem. Soc. 150 (2003) A806–A810.
[5] T. Matsumura, N. Sonoyama, R. Kanno, M. Takano, Solid State Ionics 158 (2003) 253–260.

[6] H. Morimoto, S. Tobishima, Y. Iizuka, J. Power Sources 146 (2005) 315–318.
[7] S. Ito, K. Nakaoka, M. Kawamura, K. Ui, K. Fujimoto, N. Koura, J. Power Sources 146 (2005) 319–322.
[8] S. Kanzaki, T. Inada, T. Matsumura, N. Sonoyama, A. Yamada, M. Takano, R. Kanno, J. Power Sources 146 (2005) 323–326.
[9] M. Quintin, O. Devos, M.H. Delville, G. Campet, Electrochim. Acta 51 (2006) 6426–6434.
[10] P.L. Taberna, S. Mitra, P. Poizot, P. Simon, J.M. Tarascon, Nat. Mater. 5 (2006) 567–573.
[11] S. Kanzaki, A. Yamada, R. Kanno, J. Power Sources 165 (2007) 403–407.
[12] P.C. Wang, H.P. Ding, T. Bark, C.H. Chen, Electrochim. Acta 52 (2007) 6650–6655.
[13] M. Rosso, C. Brissot, A. Teyssot, M. Dolle, L. Sannier, J.M. Tarascon, R. Bouchet, S. Lascaud, Electrochim. Acta 51 (2006) 5334–5340.
[14] B.T. Hang, I. Watanabe, T. Doi, S. Okada, J. Yamaki, J. Power Sources 161 (2006) 1281–1287.
[15] B.T. Hang, T. Doi, S. Okada, J. Yamaki, J. Power Sources 174 (2007) 493–500.
[16] S. Laruelle, S. Grugeon, P. Poizot, M. Dolle, L. Dupont, J.M. Tarascon, J. Electrochem. Soc. 149 (2002) A627–A634.
[17] S. Grugeon, S. Laruelle, L. Dupont, J.M. Tarascon, Solid State Sci. 5 (2003) 895–904.
[18] M.M. Thackeray, W.I.E. David, J.B. Goodenough, Mater. Res. Bull. 17 (1982) 785.
[19] M.M. Thackeray, W.I.E. David, J.B. Goodenough, Solid State Chem. 55 (1984) 280–286.